Response of square honeycomb core sandwich panels to granular matter impact

Anne Kyner , Kumar Dharmasena , Keith Williams , Vikram Deshpande , Haydn Wadley

PII: S0734-743X(17)30905-3
DOI: 10.1016/j.ijimpeng.2018.02.009
Reference: IE 3073

To appear in: *International Journal of Impact Engineering*

Received date: 23 October 2017
Revised date: 24 January 2018
Accepted date: 23 February 2018

Please cite this article as: Anne Kyner , Kumar Dharmasena , Keith Williams , Vikram Deshpande , Haydn Wadley , Response of square honeycomb core sandwich panels to granular matter impact, *International Journal of Impact Engineering* (2018), doi: 10.1016/j.ijimpeng.2018.02.009

Highlights

- The out of plane displacement of edge restrained, grade 304 stainless steel sandwich panels has been measured after impact by rapidly expanding spherical shells of water saturated granular media at various velocities.
- The radial expansion of the spherical shells was imaged using high-speed video techniques and the radial velocity shown to vary from 500 to1200 m/s. The impact pressure and transmitted impulse were also measured using a Kolsky bar positioned at a symmetric location to the panel center.
- Discrete particle-based simulations successfully predicted particle front positions, velocities, impact pressures and plate deformations.
- The study has confirmed recent predictions that the panels out of plane displacement would be less than that of an equivalent solid plate provided the deflection did not exceed the panel thickness.

Response of square honeycomb core sandwich panels to granular matter impact

Anne Kyner, Kumar Dharmasena, Keith Williams*, Vikram Deshpande** and Haydn Wadley

Department of Materials Science and Engineering, University of Virginia, Charlottesville, VA 22903, USA

*Newtec Services, Edgefield, SC, USA

** Engineering Department, Cambridge University, UK

Abstract

The deformation of square honeycomb core, stainless steel sandwich panels by the impact of explosively accelerated granular matter has been investigated and compared to results from a previous study using equivalent (same material and mass per unit area) solid plates subjected to similar impulsive loadings. Spherical explosive charges surrounded by 25-150 kg mass annular shells of water-saturated granular media (either fused silica or zirconia particles) were suspended above the center of the edge clamped test panels. The radially expanding granular particle front velocities were measured from high-speed video images, and revealed that the granular matter had been accelerated to velocities of 500-1200 m/s after detonation. A Kolsky bar was used to measure the time-dependent pressure and impulse at a position equivalent to the panel center, while the permanent deflections of the sandwich panels were determined by profilometry after the experiments. Even though fracture of electron beam welds used to attach the back face sheet to the sandwich panel core occurred in all the tests, the permanent deflections of the sandwich panel back faces were significantly less than those of equivalent solid plates, and were accompanied by minimal core compression. Discrete particle simulations of the granular matter acceleration and impact loading of the sandwich panels indicated that their superior deflection benefit arose from their high bending resistance rather than particle-structure interactions. This benefit was offset when the rear face of the sandwich was kept the same distance from the impulsive source as that of the solid plate since the impact face of the sandwich panel was closer to the impulsive source, subjecting it to a higher impulse than the solid plate. However, a substantial deflection reduction was still achieved by use of a strong core sandwich design.

Key words: impulsive loading, discrete particle simulations, sandwich panel, granular media

Communicating Author: Anne Kyner

1 Introduction

The deformation of structures resulting from nearby explosions has been a topic of considerable research interest for many years [1-6]. The problem's complexity arises from the difficulty of precisely predicting or measuring the impulsive loads applied to a structure by an explosive event, and the theoretical challenges associated with calculating the structure's resulting time dependent deformation and fracture. For example, the same explosive event applies quite different time dependent loads when it occurs underwater, in air, or is covered (buried) by soil. This arises from differences in the mechanisms by which momentum is transferred from the detonation event to the medium by which it is propagated towards a structure, and by subsequent interactions with the impulse-transporting medium and the structure's dynamic motion during momentum transfer.

Fundamental work by Taylor [7] and by Cole [8] investigated the effects of the dynamic motion of a structure as an underwater propagated shock front impacted a free plate. They showed that if the plate had sufficiently low inertia, it could be displaced during the shock front interaction, and both the reflected impulse and that applied to the structure were reduced. Numerous studies subsequently sought to exploit this fluid structure interaction (FSI) effect through use of sandwich panels with light impact-side face sheets and compressible (but stretch resistant) cores [9-13]. The objective was to permit out-of-plane deflection of the impact face during shock loading while reducing macroscopic bending of the sandwich panel due to its high flexural rigidity and resistance to stretching [9-11]. Significant benefits were identified for some sandwich panel designs subjected to model underwater explosive events [9, 14-19].

The studies of Taylor and Cole were recently extended to air blast loading by Kambouchev et al. [20] and by Hutchinson [21]. Their work addressed the non-linear effects activated by strong air shocks, and indicated that an analogous reduction in the shock reflection coefficient, and therefore momentum transfer to a structure, could be achieved by the use of very light structures. However, the practical implementation of this result was more difficult to exploit because it required the use of very thin/low density structures during exposure to strong shock overpressures, making it likely that such structures would rupture during shock loading [12, 22]. Even though the FSI benefit for air shock loading is smaller than in water [12, 16, 20, 23],

sandwich panel structures have been designed that sustained smaller deflections than equivalent (mass and material) monolithic plates during exposure to high intensity air shocks [13]. However, this was primarily a consequence of the higher bending resistance of a well-designed sandwich panel rather than an FSI effect [12, 13]. To exploit the sandwich panel benefit, tests must usually be restricted to regions of loading where the out-of-plane panel deflections are less than the core thickness of the sandwich panel, favoring the use of strong core topologies such as the square honeycomb [13]. For larger deflections, the structural response of the panels becomes stretching dominated, and the sandwich panel benefit over the monolithic plate diminishes or even reverses for some core topologies (such as the pyramidal lattice) [9, 13]. Ideal core designs for underwater and air shock mitigation are therefore different, since the former is optimized by provision of sufficient core crushing to enable impulse reduction by the FSI effect, while the latter requires a strong core that maintains the face sheet separation necessary to maintain bending resistance [9, 13, 16].

When an explosion occurs within a granular medium such as soil, the majority of the momentum of the explosive detonation products is transferred to the soil particles which can then attain a high velocity if their mass per unit area is low (by shallow burial) [24, 25]. The momentum that is transferred to a nearby structure by these particles is governed by momentum conservation, and it therefore depends upon the incident and reflected particle velocities. Liu et al. [26] used a particle based simulation method to investigate the normal impact of sand slugs against (solid) monolithic plates, Figure 1(a). They found that particle impacts normal to a flat surface were very weakly reflected, and the transferred impulse was approximately (within 2%) that of the incident granular matter. Their study showed that the out-of-plane deflection of a normally impacted, edge clamped monolithic plate was an approximately linear function of the applied impulse.

Even though no significant FSI effect existed, the study found that equivalent sandwich panel designs (of equal mass per unit area to the monolithic plates), Figure 1(b), outperformed their monolithic counterparts, and the benefit increased when a high normalized strength core was utilized, Figure 1(c). In Figure 1(c), the normalized core strength was given by,

$$\text{normalized core strength} = \frac{\sigma_c^*}{\sigma_{face}} \qquad (1)$$

where σ_c is the core compressive strength, σ_y is the yield strength of the solid from which the core was made, and $\bar{\rho}$ is the relative density of the cellular core. Additional reductions in panel deflection were observed for sandwich panels with low aspect ratio (thick core and small span between loading points) and higher flexural stiffness. Since the small FSI effect did not result in significant variations in transferred impulses [26-28], the primary benefit of a sandwich panel subjected to impact by granular media resulted from the panel's high bending resistance [16, 26-28].

Subsequent experimental and particle-based simulation studies of explosively accelerated sand particle impact with high aspect ratio, weak (corrugated) core aluminum sandwich structures have shown that rapid dynamic deflections of low strength sandwich panel systems can induce very strong particle reflections that locally amplify the impulse applied to the structure [29]. For example, since the webs of a corrugated core are compressed slowly, compared to the rate at which the face sheet suspended between them suffers out of plane displacement, sand particles can be strongly reflected out of the plane of the overall panel from the local concavities. The resulting local amplification of impulse then leads to an instability resulting in local rupture of the face sheet near hard points. This study also showed that panel deformation and impulse amplification also occurred near lower strength (and ductility) welds. Very strong impulse amplification can also occur when reflected sand particles travelling parallel to the impacted surface are reflected out of the panel plane by picture frame-type grips that extended above the plate surface. This out-of-plane reflection induces a reaction momentum that promotes shear-off failure at the attachments [29].

This prior work identified several design principles for sandwich structures intended for high intensity granular impact mitigation. Firstly, they should utilize a strong, stretch resistant core in combination with a sufficiently thick impact face sheet that large dynamic displacements between core nodes are avoided. Square honeycomb cellular cores are ideal candidates for the core since they have both a high compressive strength and excellent in-plane stretching resistance [11, 13, 16, 30-33]. Second, the use of welds on the impact side faces should be avoided. Third, panels should provide a flat, smooth surface for uninterrupted flow of reflected particles across the structures impact surface. Finally, Figure 1 shows that the fabrication of panels from materials with a high value of $\alpha_{shock}\sqrt{\sigma_y / m_b}$ (where m_b is the panel mass per unit

area, σ_y is the material yield strength and ρ its density) is preferred, provided a higher value of yield strength does increase the susceptibility to rupture.

The objective of the study described here is to determine if a strong core sandwich panel concept can reduce the structural deflection following impact by high velocity granular matter. The recently reported [34] out-of-plane displacements of large area, 2.54 cm thick square 304 stainless steel monolithic (solid) plates impacted by radially expanding fused silica or zirconia particle shells accelerated to velocities of 500-1,200 m/s are used for a solid plate reference response. In these reference tests, a Kolsky bar was used to measure the pressure and impulse at an equivalent location to the center of the plates during five experiments of increasing incident impulse. The permanent plastic displacement of the solid plates was measured as a function of the maximum impulse and shown to scale linearly with impulse consistent with the recent analysis of Liu et al. [26]. The study presented here investigates the permanent deformation and dynamic displacements of equivalent (same mass per unit area), square honeycomb core sandwich panels made of the same 304 stainless steel alloy used for the reference study, after they were subjected to similar high intensity granular impact [34]. In the current study, the displacements and Kolsky bar pressure and impulse waveforms for the five experiments are simulated using the IMPETUS Afea discrete particle simulation code. This simulation approach was then used to analyze the plate's dynamic response. The experimental and simulation results confirm a significant reduction of the panel deflection when the mass of a solid plate is redistributed as a strong core sandwich panel. However, this benefit is reduced if the rear face of the sandwich is kept the same distance from the impulsive source as that of the solid plate. In this case, the greater panel thickness places the impact face closer to the impulsive source, subjecting it to a higher impulse than the solid plate.

2 Experimental setup

The experimental tests were conducted at the same outdoor blast testing facility (NEWTEC Services Group Inc., Edgefield, SC) used to evaluate the solid plate reference responses [34]. The 5.08 cm thick square honeycomb core sandwich panels were edge clamped to the same test platform as the (2.54 cm thick) solid plates. A schematic illustration of the overall test arrangement is shown in Figure 2. The test platform consisted of a steel picture frame to support

the target panels, a suspended spherical test charge consisting of a spherical explosive core and annular shell of water-saturated fused silica or (higher density) zirconia particles, and a strain gauge instrumented Kolsky bar to measure the applied pressure and impulse during granular particle impacts. A brief description of the test platform, charge configuration, and Kolsky bar system is given below. Full technical details can be found in Kyner et al. [25, 34].

Figure 3 schematically illustrates the test configuration geometry for the two types of targets. It shows the concentric spherical charge suspended above the center of the test targets. The charge consisted of an internal sphere of radius R_1 packed with composition C-4 explosive, surrounded by an outer sphere of radius R_2 filled with water-saturated fused silica or zirconia particles. The applied impulse was varied by changing R_1 and R_2 and the type (density) of the granular matter. Since the impulse applied to a test structure also varies with standoff distance, we attempted to use a standardized distance. The tests could have been conducted with a fixed target front (impacted) face to charge center distance or with a fixed distance from the charge center to the target back face. For the latter, the front face of the thicker sandwich structure would be closer to the charge center, and therefore suffer a higher impulse. Since this is a more conservative test of the sandwich panel benefit, an intended constant standoff distance, H_b = 47.54 cm, from the center of the test charges to the back face of both target types was attempted, as shown in Figure 3. As a result, the intended distance from the center of the test charge to the front face of the sandwich panel would be H_p = 42.46 cm while that to the front face of the solid plate would have been 45 cm. In practice, small variations in the actual standoff distances from the intended values occurred as described below.

2.1 Test platform

The test platform was identical to that used for the testing of the five reference solid plates [34]. Figure 2 shows a schematic illustration of the full test setup. A honeycomb sandwich panel is shown in Figure 3 positioned on the picture frame support base with the spherical test charge suspended above. Two high-speed cameras (Vision Research Inc., Phantom V7.3) captured the granular (sand) front position for each test shot as they radially expanded towards the Kolsky bar and test panel after detonation. The front 1.32 m length of the test panels and a 10 cm length for Shots 1 and 2 (15 cm for Shots 3-5) at the front of the Kolsky bar were spray-painted prior to testing to provide reference lengths for interpreting the high-speed video images.

2.2 Honeycomb panel design and fabrication

Square honeycomb core sandwich panels were used for the tests since this core has a high compressive strength, and resists in-plane stretching during panel bending [9, 35]. To ensure the compressive strain during the tests would be small, a core relative density, "ρ "ρ"ρ, of 30% was selected ("ρ is the smeared-out core density and "ρ the material density of the stainless steel [30]). The honeycomb core density "ρ "ρ"ρ for a core made from 304 stainless steel with material density "ρ = 7900 kg/m^3 was therefore 2370 kg/m^3. The sandwich panels were designed to have the same mass per unit area as the reference 304 stainless steel solid plates. Approximately a third of the solid plate mass was assigned to the core with the remainder distributed between the 7.9 mm thick front and 6.4 mm thick back face sheets. A slightly thicker impact face sheet was used to increase its bending resistance in the unsupported region between contacts with the core webs. Figure 4(a) shows a photograph of the core while Figure 4(b) and (c) show the top and section views of the square honeycomb core pattern. The sandwich panel design parameters are summarized in Table 1.

Table 1. The design parameters for the square honeycomb sandwich panels.

Cell width D (mm)	Web width t (mm)	Unit cell width l (mm)	Core height H_c (mm)	Front face thickness t_f (mm)	Back face thickness t_b (mm)	Panel thickness t_p (mm)	Corner radius r (mm)
44.45	6.35	50.80	36.50	7.90	6.40	50.80	9.50

The sandwich panels were fabricated from 1.32 m x 1.32 m x 7.6 cm thick 304 stainless steel plates that were first stress relieved at Rex Heat Treat (Warrendale, PA) at 538° C for eight hours and then machined at KVK Precision Technologies (Shenandoah, VA). This was the same steel and stress relief process used for the fabrication of the five solid (reference) test plates [34]. A 1.22 m x 1.22 m and 2.54 cm deep center pocket was first milled out of the plate to form a 5.08 cm wide picture frame outer edge. This allowed the panels to fit tightly over the test platform support base resulting in an edge restraint condition without interrupting subsequent flow of the granular particles over the impact surface. To avoid welding of the honeycomb core to the impact side face sheet of the sandwich panel, a 16 x 16 square array of 44.45 mm x 44.45 mm square cell pockets was milled in the center 81.3 cm x 81.3 cm square span of the panel. The centers of the cells were spaced 50.8 mm apart and each had a depth (i.e. core height, H_c) of

36.5 mm. To minimize stress concentrations, the corners and bottoms of the cell pockets were rounded to a 9.5 mm radius using a ball mill cutter as shown in Figure 4(b). The integral front (impact) face sheet was 7.9 mm thick. The integral face sheet/core structure had a total thickness ($H_c + t_f$) of 44.4 mm, Figure 4(a). A thinner 1.22 m x 1.22 m back face sheet with thickness t_b = 6.4 mm was then attached by electron beam welding at Sciaky, Inc. (Chicago, IL) to form the complete square honeycomb sandwich panel structure with a total thickness (panel height) of t_p = 50.8 mm.

A linear welding scan pattern in the orthogonal X- and Y- directions was adopted for welding at each of the honeycomb web and back face sheet intersections. Since the honeycomb cell matrix pattern was only defined in the center square 81.3 cm x 81.3 cm unsupported area, a series of additional perimeter welds were used to cover the area between the inner honeycomb cell matrix pattern and the outer picture frame edges, as shown in Figure 5. Electron beam weld parameters were first developed for the through thickness welding of small test coupons with a representative T-joint configuration consisting of a 6.4 mm thick face sheet and a 6.35 mm wide honeycomb web. This resulted in selection of an electron beam welding voltage of 50 kV and a 100 mA beam current with a travel speed 38.1 mm/s. The weld varied in width from 0.51 to 0.64 mm and had a total penetration depth of 10.16 mm. Since the back face sheet was 6.4 mm thick, the weld penetrated about 3.76 mm into the honeycomb core web. The use of a narrow weld width was necessary to avoid excessive thermal stress, and thus distortion of the panels. It is shown later that the rupture strength of these welds was insufficient to withstand the dynamic loading conditions of this test series.

2.3 Test charges

The five test charges were identical to those for the solid test plate study [34]. Their designs are summarized in Table 2. A carbon fiber reinforced polymer (CFRP) suspension rod, inserted through the center of the test charges during assembly, was used to assist in the suspension and alignment of the charges above the test panels. The three highest mass test charges (Shots 3-5) required the additional use of a net for their suspension. In order to create a similar impulse at the Kolsky bar to that at the plate center, the location of detonation on the explosive charge surface was inclined at $\theta = 45°$ from the test panel normal on the plane that contained the center axis of the Kolsky bar and test plate centerline, Figure 6. Positioning these heavy test charges in

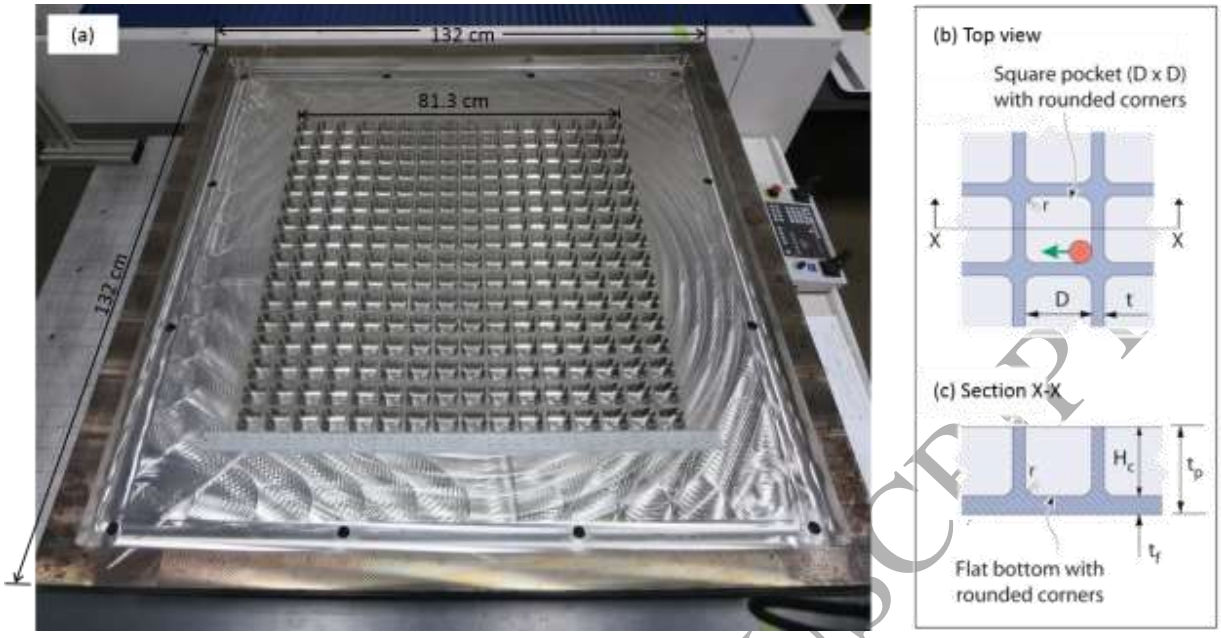

Figure 4 (a) A photograph of the square honeycomb core sandwich panel before the back (bottom) face sheet was attached. The square honeycomb pockets were machined from a thick plate so that the impact side face sheet did not require bonding with the core structure. (b) Shows a schematic view of the cells viewed from above. (c) Shows a schematic illustration of the connection between the front face sheet and the core webs.

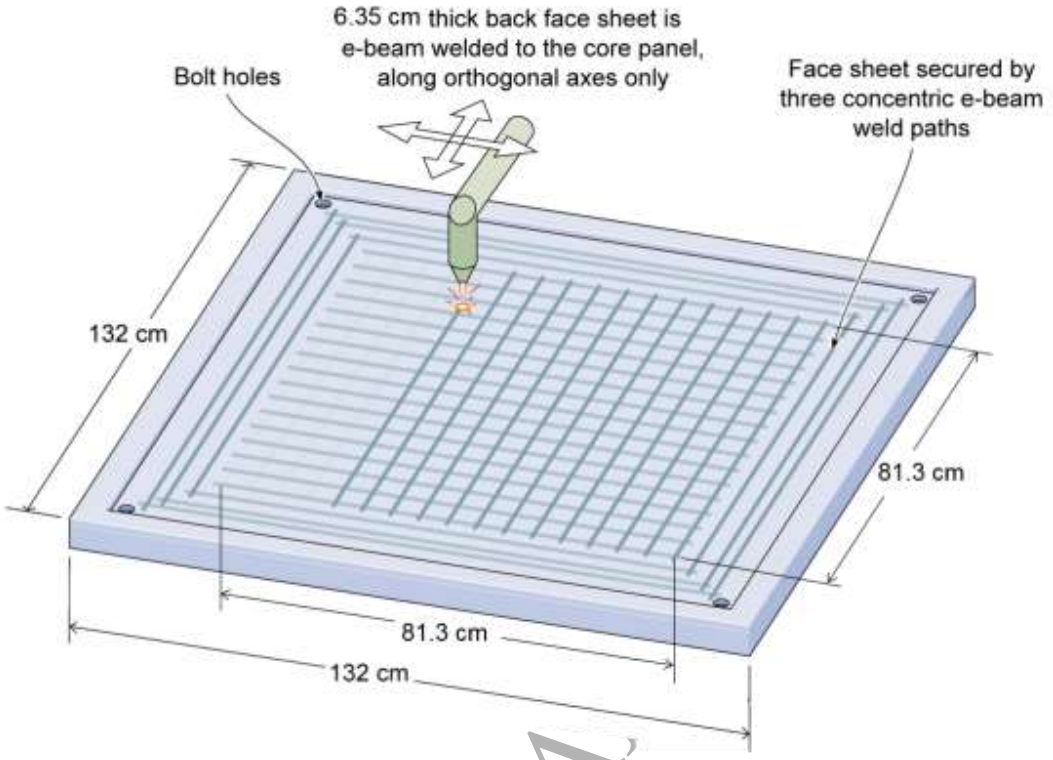

Figure 5 The linear electron beam welding pattern used for attachment of the back face sheet. Each weld line penetrated the back face sheet and center of each honeycomb web to a depth of 3-4 mm. Additional weld lines were used to attach the back face sheet to the 20.3 cm wide solid panel region outside the honeycomb core.

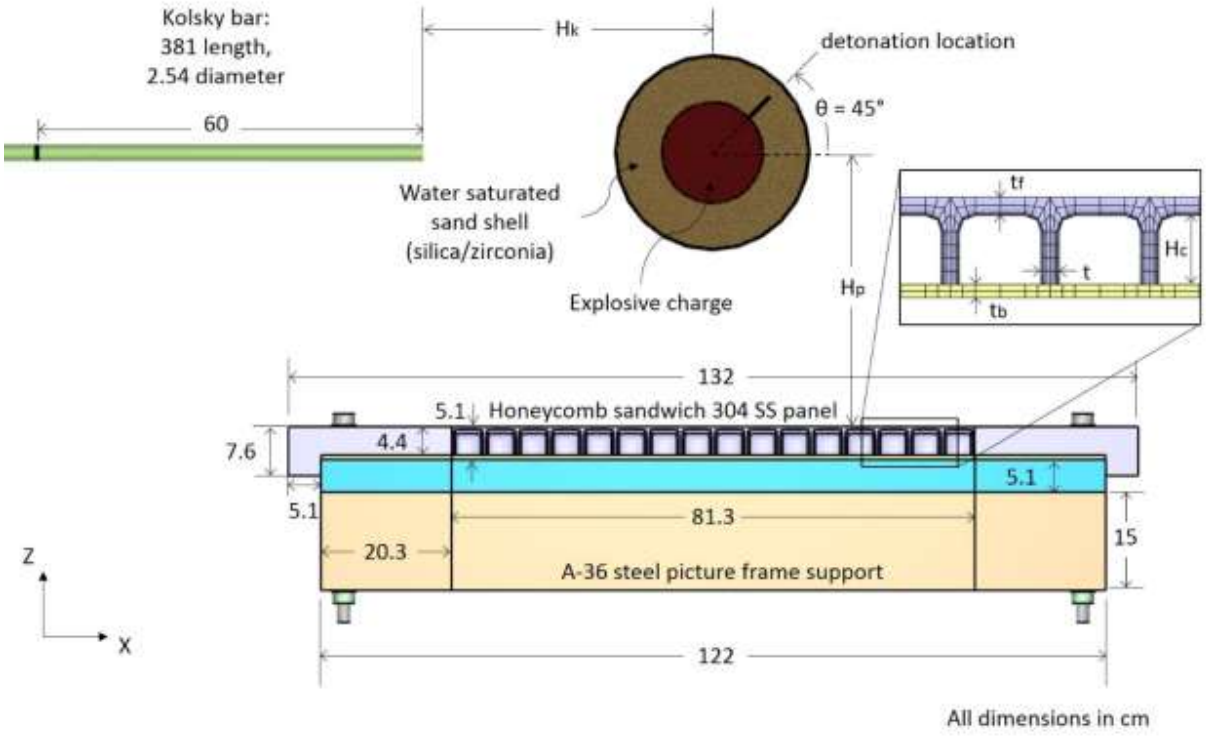

Figure 6 Cross section of the model geometry used for simulations of the tests with an inset showing the mesh used for the honeycomb core and back face sheet.

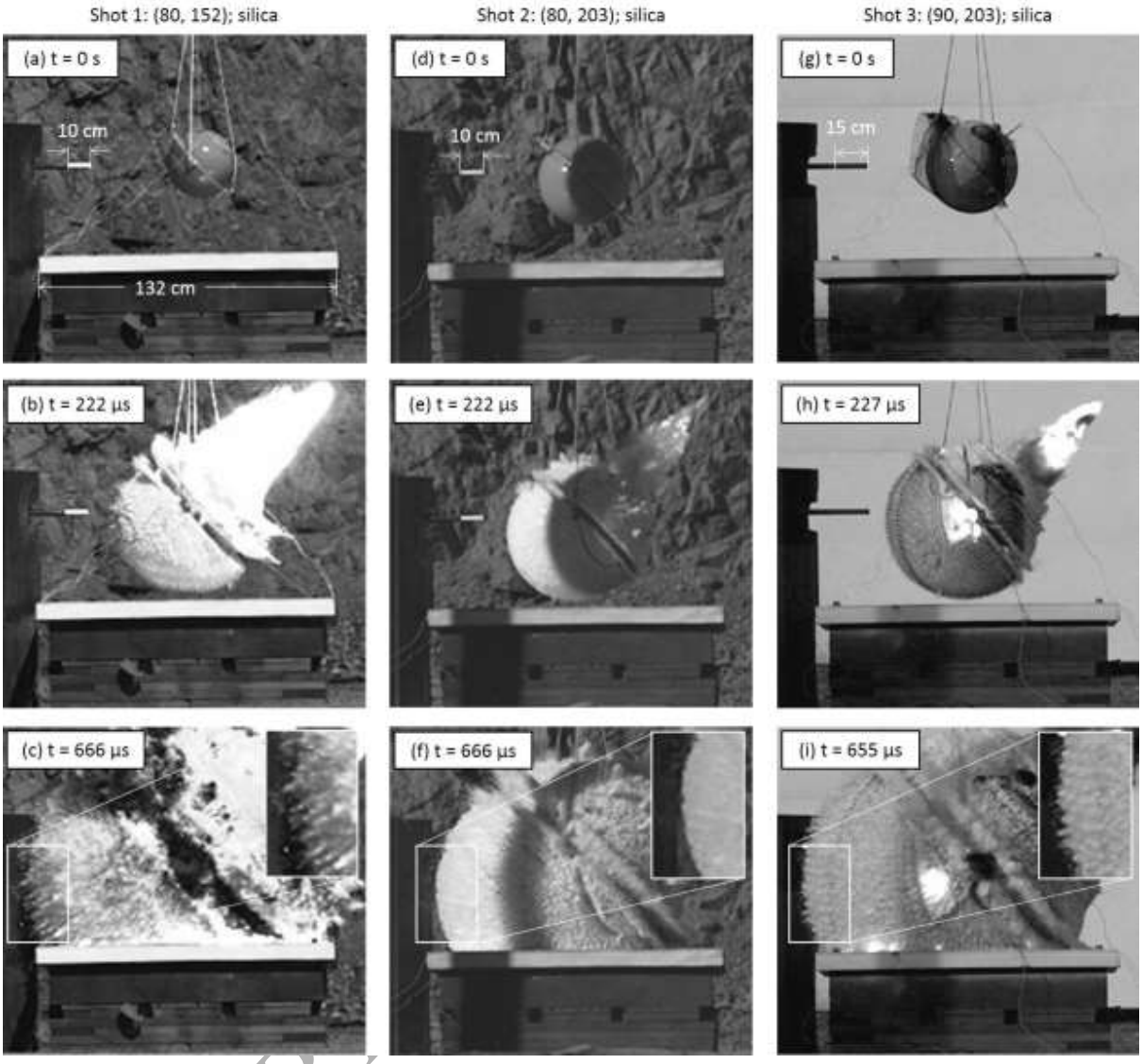

Figure 7 Fused silica microsphere tests with square honeycomb sandwich panels showing approximately equivalent time snapshots for Shot 1 (R1 = 80 mm; R2 = 152 mm; 3 kg explosive charge), Shot 2 (R1 = 80 mm; R2 = 203 mm; 3 kg explosive charge), and Shot 3 (R1 = 90 mm; R2 = 203 mm; 4.5 kg explosive charge).

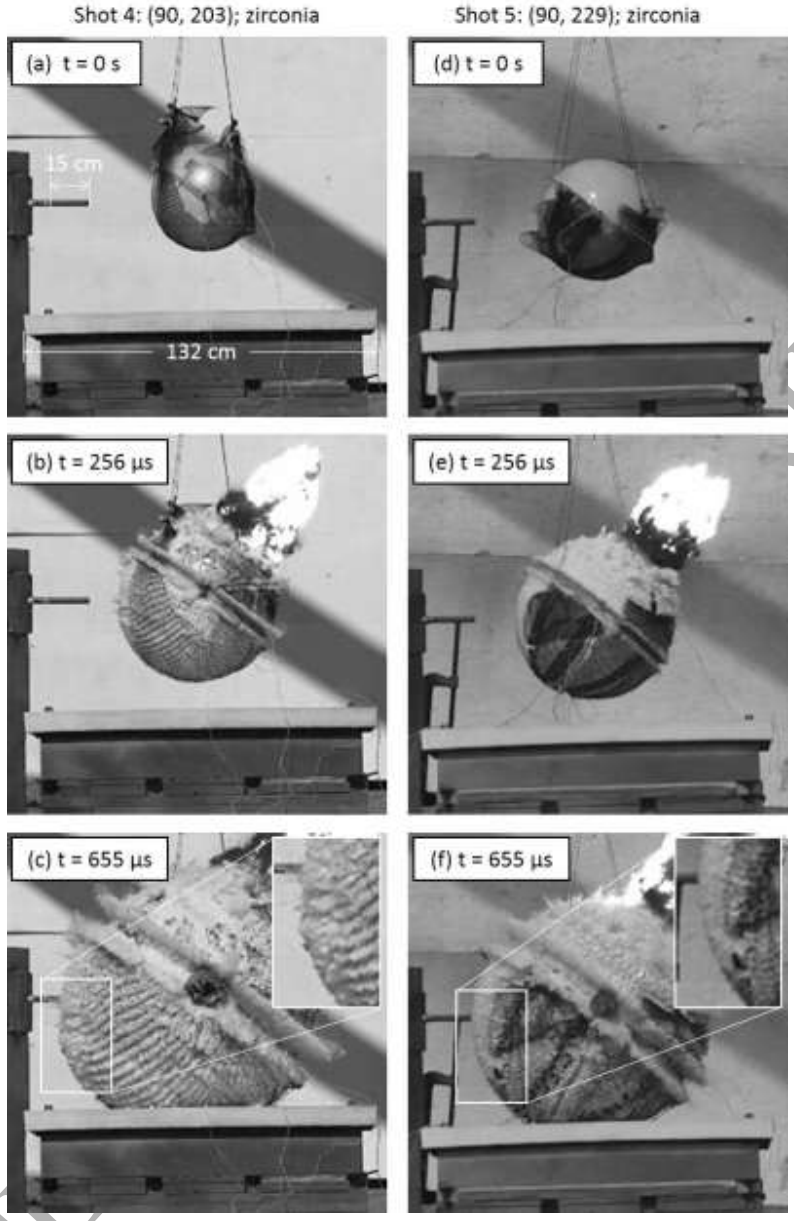

Figure 8 Zirconia particle tests with square honeycomb sandwich panels showing approximately equivalent time snapshots for Shot 4 (R1 = 90 mm; R2 = 203 mm; 4.5 kg explosive charge) and Shot 5 (R1 = 90 mm; R2 = 229 mm; 4.5 kg explosive charge).

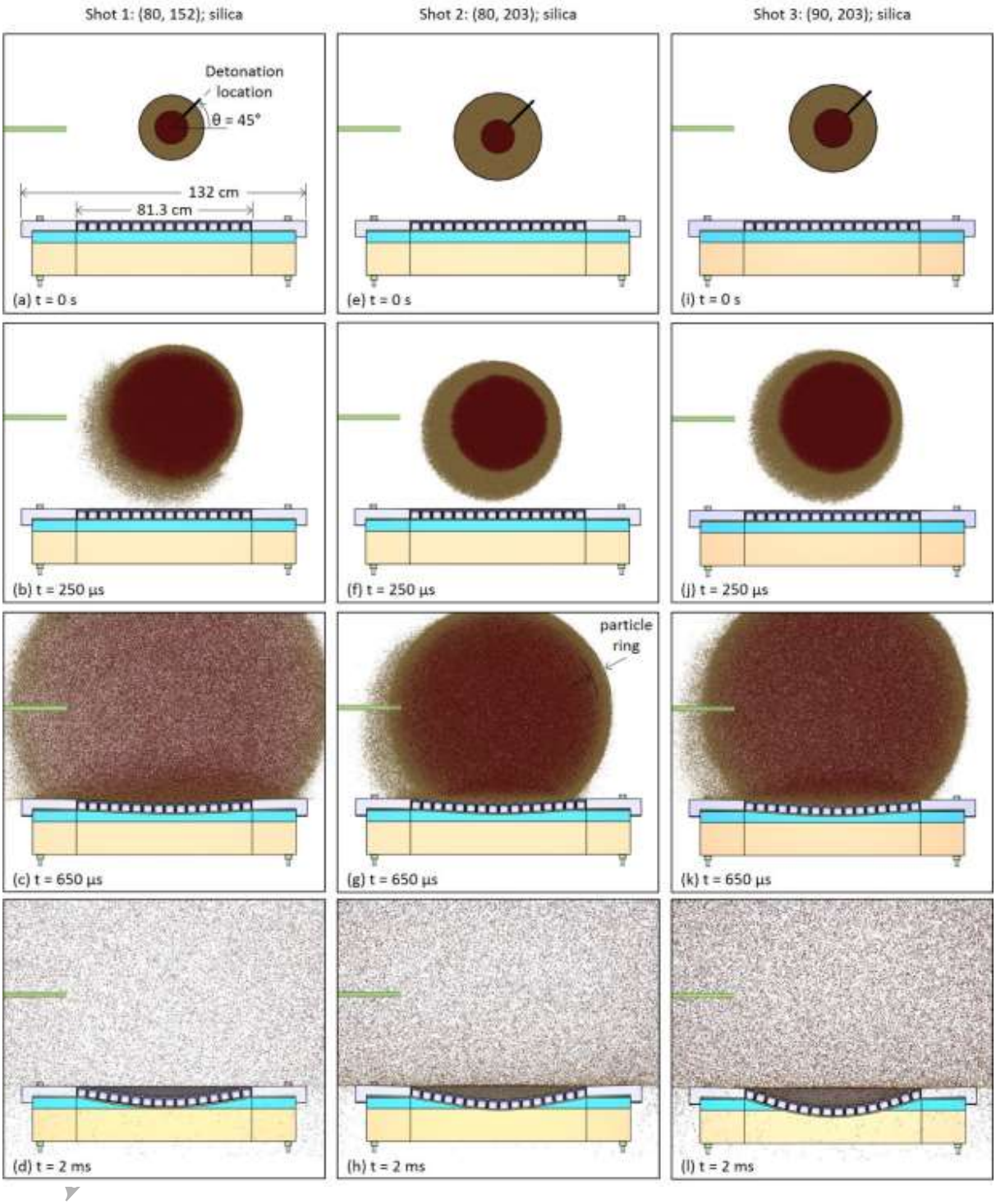

Figure 9 Simulated sand front propagation for the three fused silica particle tests (Shots 1-3) for t = 0 s (the moment of detonation), t = 250 >s, t = 650 >s, and t = 2 ms. The silica particles are tan while the inner red particles are those of the high explosive.

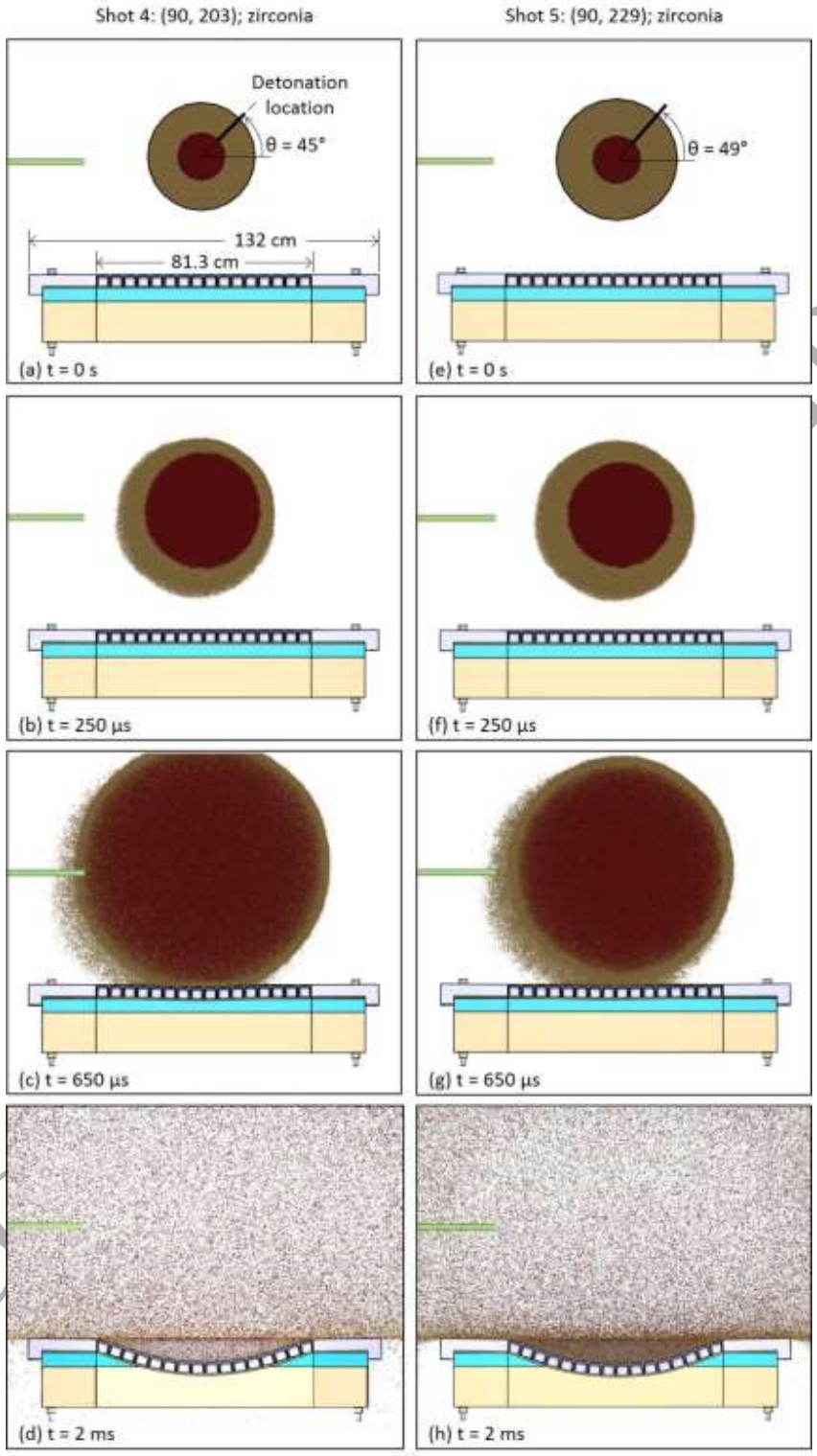
Shot 4: (90, 203); zirconia
Shot 5: (90, 229); zirconia
Detonation location
θ = 45°
132 cm
81.3 cm
θ = 49°
(a) t = 0 s
(e) t = 0 s
(b) t = 250 μs
(f) t = 250 μs
(c) t = 650 μs
(g) t = 650 μs
(d) t = 2 ms
(h) t = 2 ms

Figure 10 Simulated sand front propagation of the two zirconia particle tests (Shots 4 and 5) for t = 0 s (the moment of detonation), t = 250 >s, t = 650 >s, and t = 2 ms. The zirconia particles are tan and the high explosive particles are red.

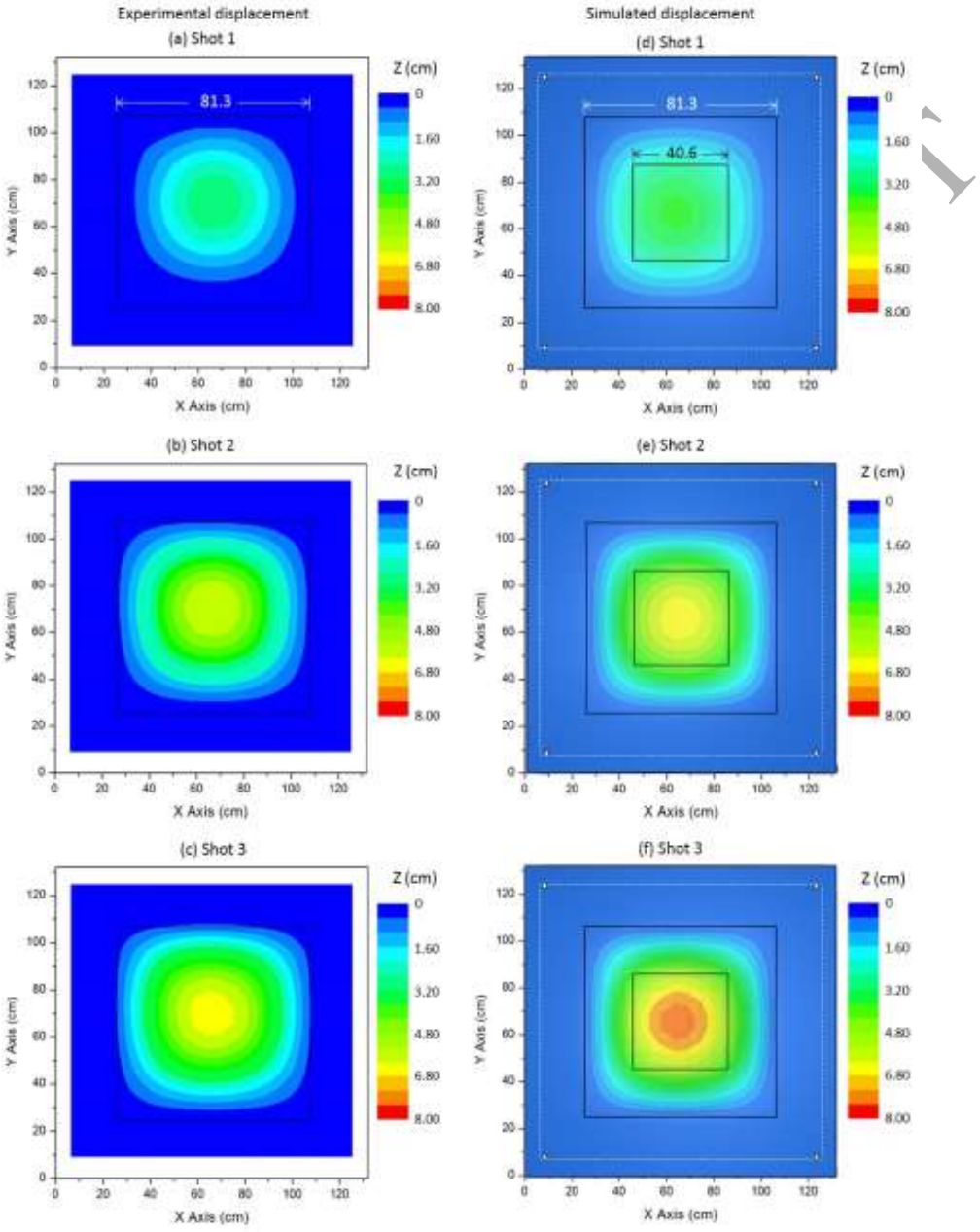

Figure 11 Test panel permanent plastic displacement contour plot in the Z direction for the silica particle tests (Shots 1-3). Experimental profilometry measurements are shown in (a), (b) and (c). These measurements did not include the outer edge (white region) of the panels. The corresponding simulated responses (evaluated at t = 20 ms) are shown in (d), (e), and (f). The 81.3 cm wide black square indicates the edge of the underlying support base and location of the

region with honeycomb cells. The inner, 40.6 cm wide black box indicates the refined mesh region used in the FE model. The 122 mm wide dashed white box in the simulation plots indicates the position of the edge grip from which displacements were determined.

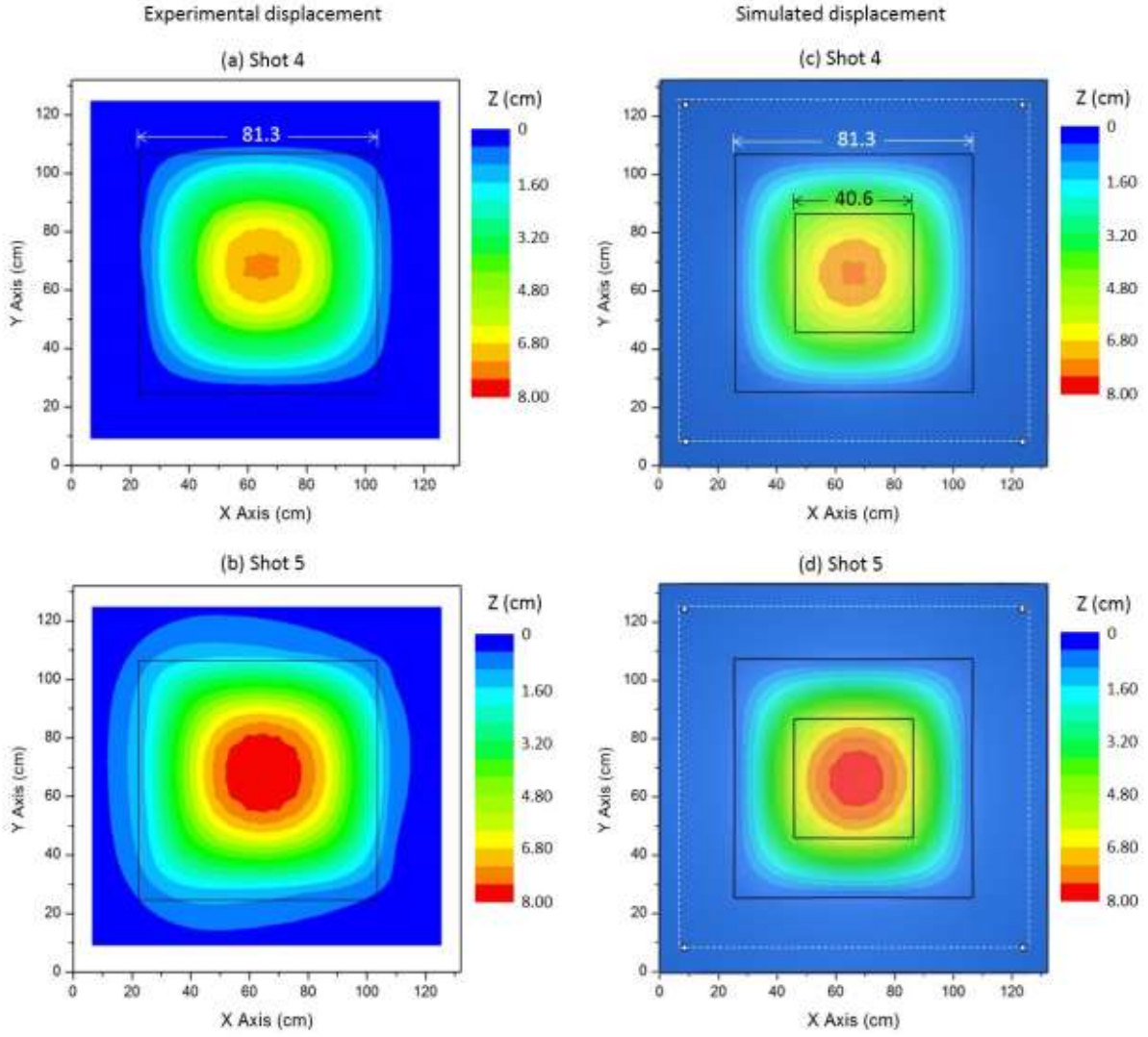

Figure 12 Test panel permanent plastic displacement contour plot in the Z direction for the zirconia particle tests (Shots 4 and 5). Experimental profilometry results are shown in (a) and (b). The simulated responses (at t = 20 ms) are shown in (c) and (d).

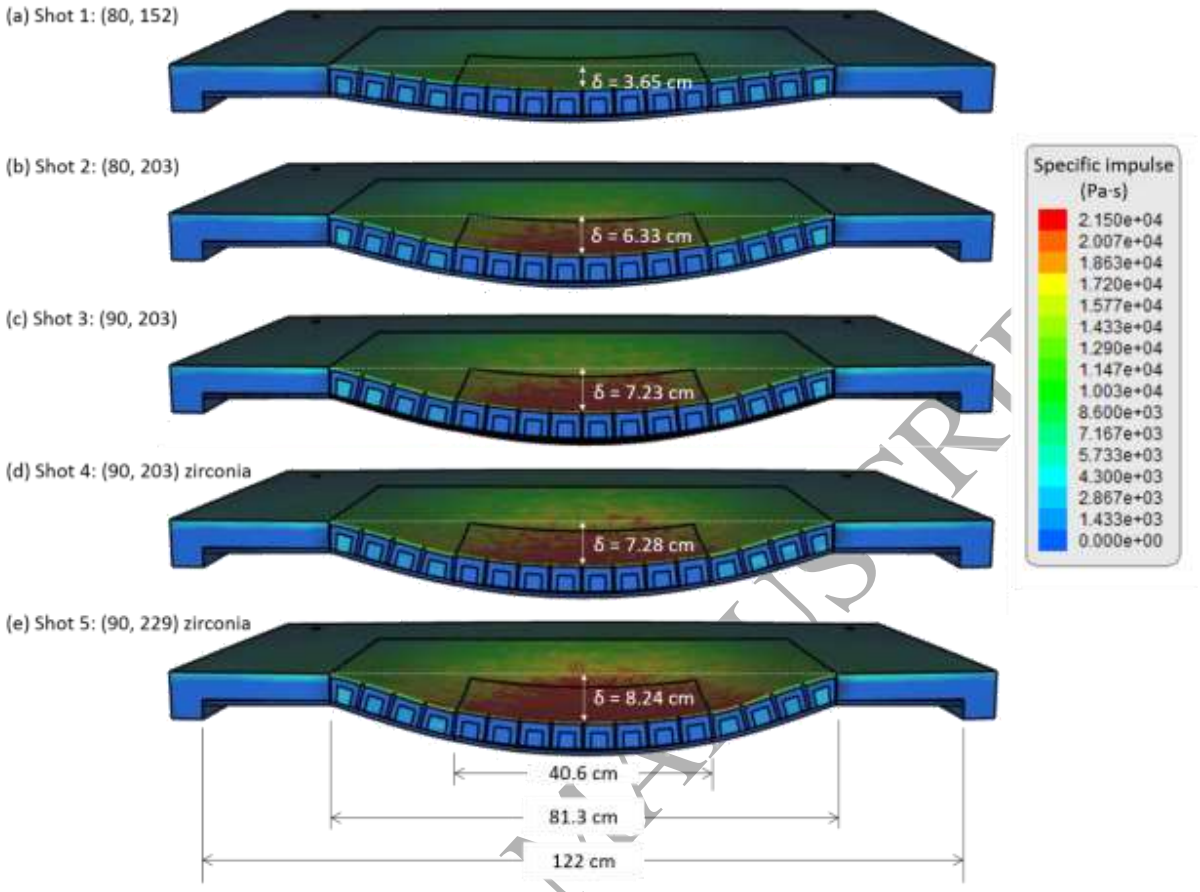

Figure 13 The cross section of the simulated square honeycomb sandwich panels showing the predicted specific impulse distribution applied to the surface by the five test shots. The 81.3 cm wide (unsupported) region of the honeycomb core sandwich section is indicated along with the 40.6 cm wide center region where a refined mesh was used. The predicted permanent deformation and permanent out of plane deflection (δ) is also shown for each test.

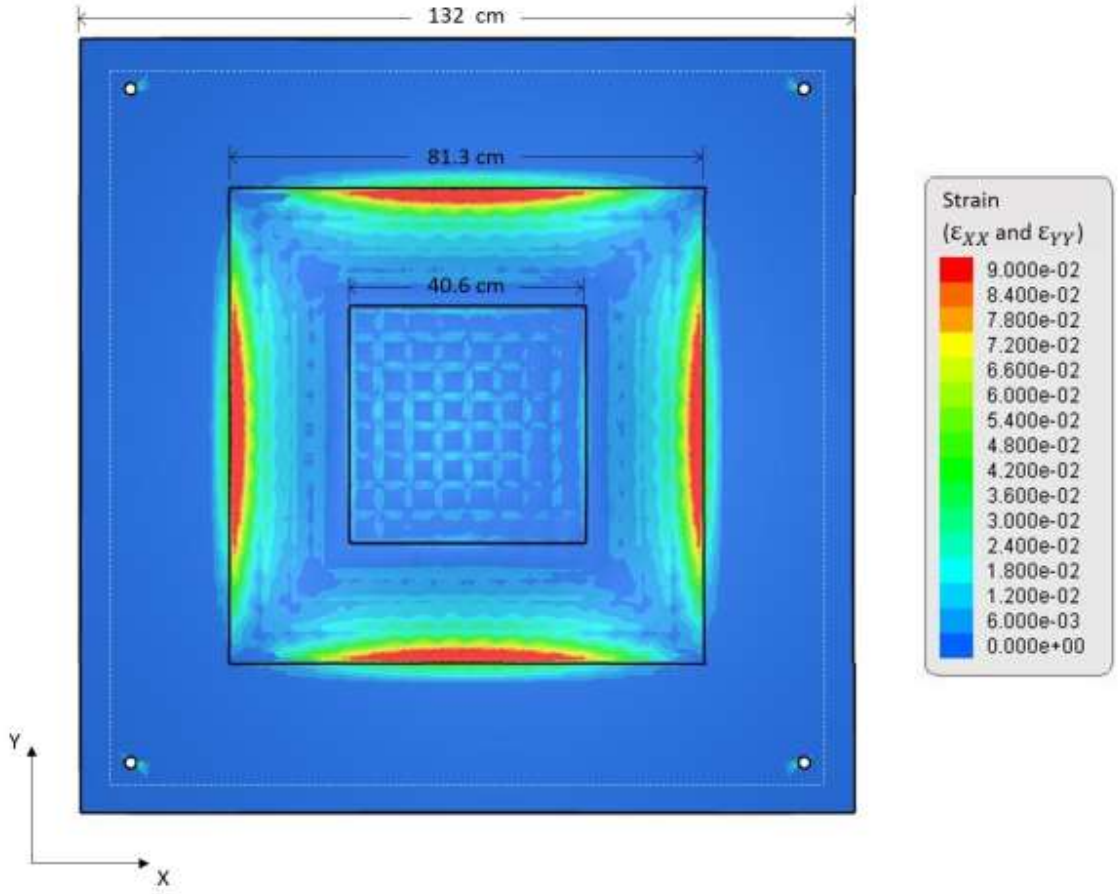

Figure 14 Superposition of the in-plane extensional strains (-, , and -, ,) on the top face of the honeycomb sandwich panel for Shot 3 after an elapsed time t = 20 ms. The dotted white box indicates the location of the 122 cm wide edge grip.

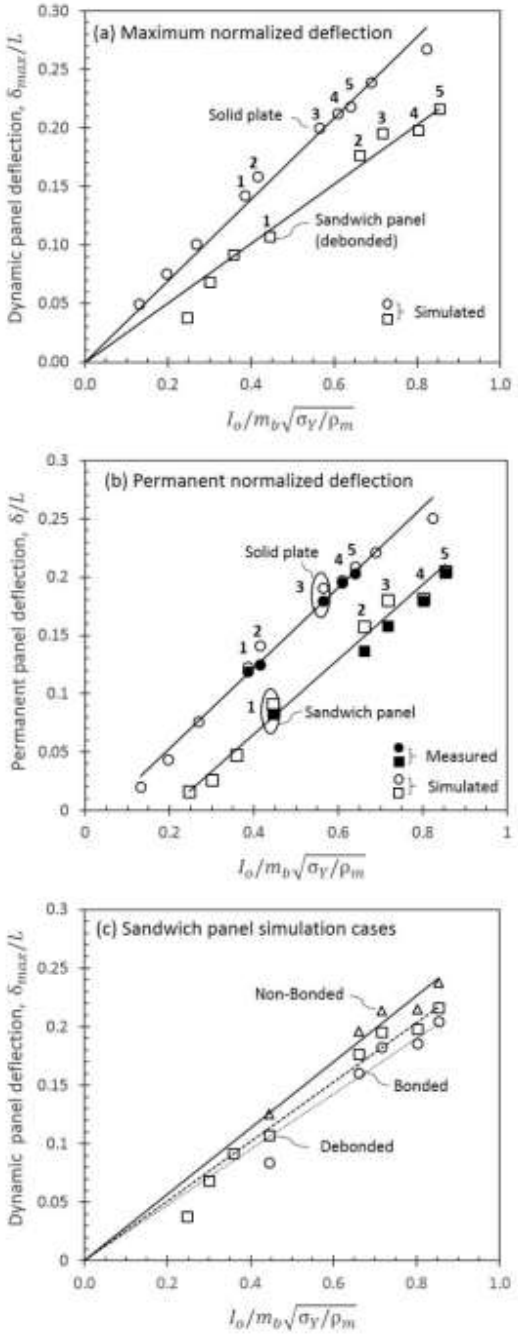

Figure 15 (a) The simulated peak dynamic displacement at the center of the sandwich panels and reference solid plates versus the applied impulse. The numbers adjacent to some data points correspond to the test shot number. The simulations permitted rear face sheet debonding during the impulsive loading of the sandwich panel. (b) The measured and simulated permanent front face displacement at the center of the test structures versus the applied impulse. The sandwich panel simulations again allowed rear face sheet debonding during the tests. (c) Shows the effect

of changing the rear face sheet attachment condition on the dynamic deflection of the sandwich panels.

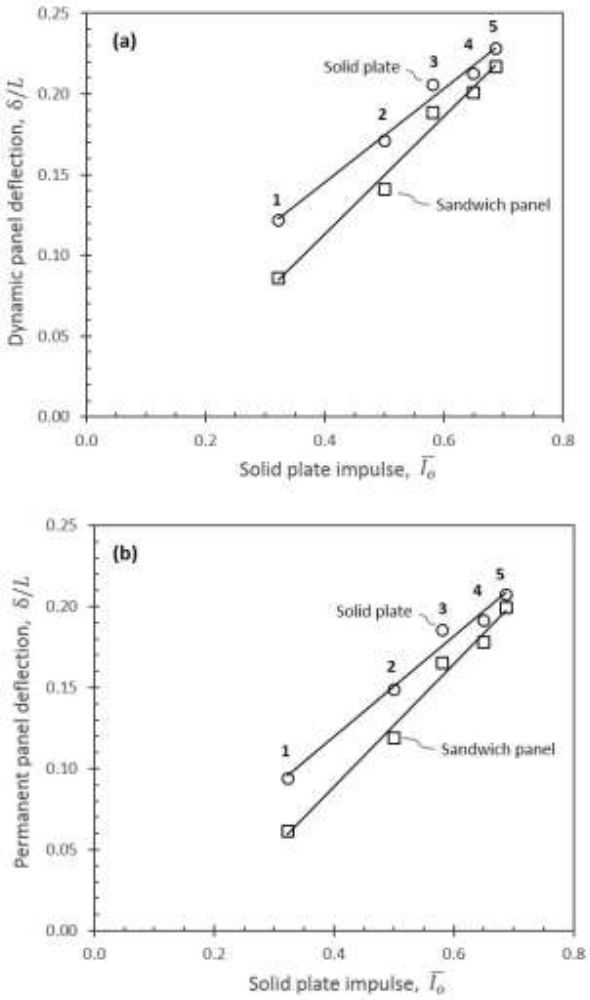

Figure 16 (a) The simulated dimensionless maximum dynamic deflections of solid plates and sandwich panels versus the dimensionless impulse applied to the reference solid plates and (b) the permanent panel deflections. Simulations were performed using a fixed standoff distance, H_b = 47.54 cm, to the back face of all the samples.

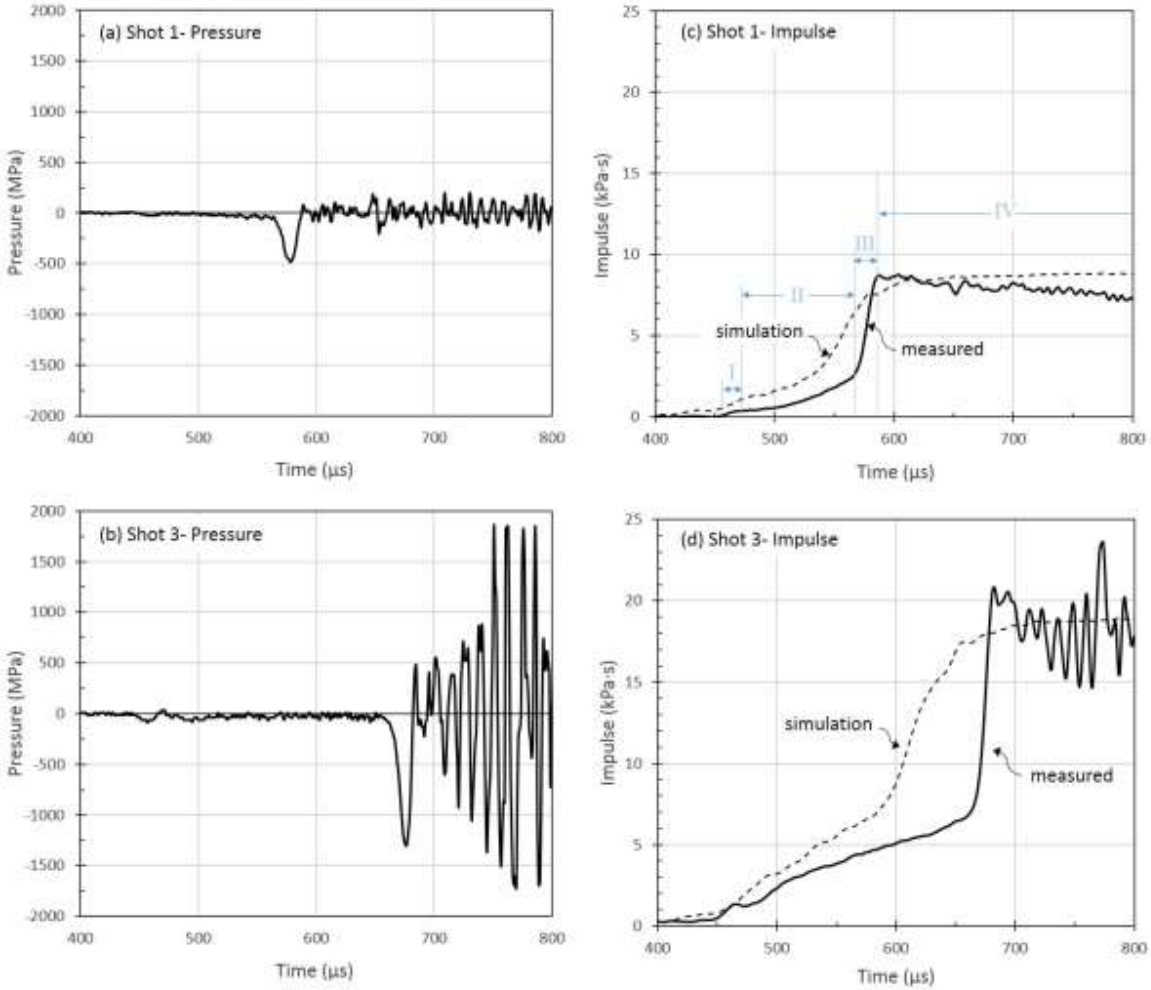

Figure A.1. Kolsky bar data for the glass microsphere particle tests. The waveforms in (a) and (b) show the pressure measured at the strain gage location for Shots 1 and 3. Figures (c) and (d) show the impulse for test Shots 1 and 3. The four regions of impulsive loading applied to the Kolsky bar are indicated in (c).

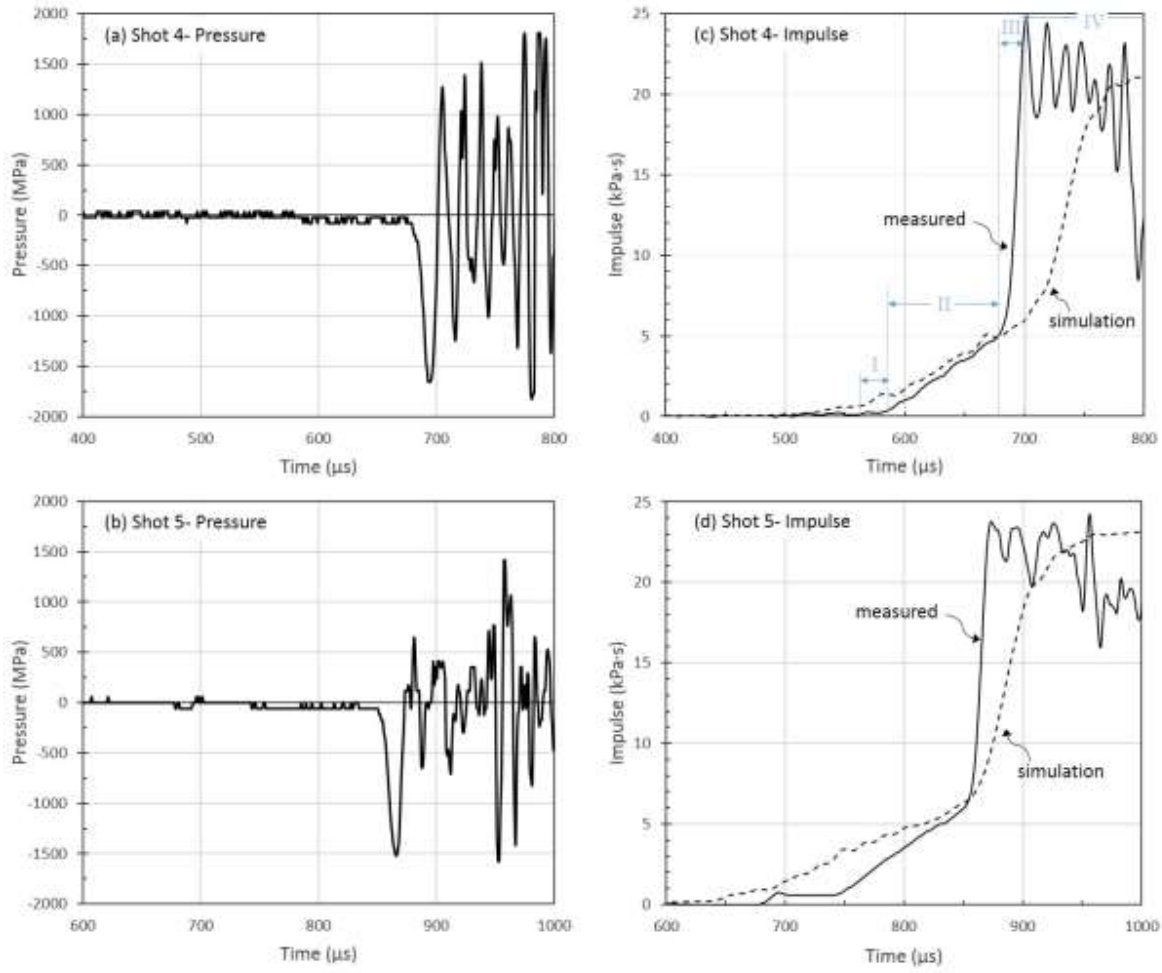

Figure A.2. Kolsky bar data for the zirconia particle tests. The waveforms in (a) and (b) show the pressure measured at the strain gage location for Shots 4 and 5. Figures (c) and (d) show the impulse for test Shots 4 and 5. The four regions of impulsive loading applied to the Kolsky bar are indicated in (c).